



Received 30 September 2022
Accepted 26 October 2022

Edited by J. T. Mague, Tulane University, USA

Keywords: nickel; nickel(II) complex; crystal structure; pyrazole; Hirshfeld surface analysis.

CCDC reference: 2215549

Supporting information: this article has supporting information at journals.iucr.org/e

Crystal structure and Hirshfeld surface analysis of dichloridotetrakis(4-methyl-1*H*-pyrazole- κN^2)-nickel(II) acetonitrile disolvate

Oleksandr S. Vynohradov,^{a*} Yuliya M. Davydenko,^a Vadim A. Pavlenko,^a Dina D. Naumova,^a Sergiu Shova^b and Denys Petlovanyi^c

^aDepartment of Chemistry, Taras Shevchenko National University of Kyiv, Volodymyrska str. 64/13, 01601 Kyiv, Ukraine,

^b"Poni Petru" Institute of Macromolecular Chemistry, Aleea Gr. Ghica, Voda 41A, 700487 Iasi, Romania, and ^cEnamine Ltd, Oleksandra Matrosova Str. 23, Kyiv 01103, Ukraine. *Correspondence e-mail: osvynohradov@ukr.net

The title compound, $[NiCl_2(C_4H_6N_2)_4] \cdot 2CH_3CN$, is a mononuclear octahedral Ni^{II} pyrazole-based complex. Two acetonitrile molecules are linked to the Ni^{II} complex by $N-H \cdots N$ hydrogen bonds. The Ni^{II} atom is octahedrally coordinated by four N atoms of four 4-methyl-1*H*-pyrazole ligands, forming the equatorial plane. The axial positions are occupied by two Cl atoms. $[NiCl_2(C_4H_6N_2)_4] \cdot 2CH_3CN$ was synthesized by the reaction of 4-methyl-1*H*-pyrazole with nickel(II) chloride hexahydrate in acetonitrile solution under ambient conditions and characterized by single-crystal X-ray diffraction analysis. A Hirshfeld surface analysis was performed, which suggests that the most important contributions to the surface contacts are from $H \cdots H$ (62.1%), $H \cdots N/N \cdots H$ (13.7%), $H \cdots C/C \cdots H$ (13.4%) and $H \cdots Cl/Cl \cdots H$ (10.1%) interactions.

1. Chemical context

Pyrazoles as ligands are widely used for the synthesis of coordination compounds because of their rich coordinative flexibility (Trofimenko, 1972; Mukherjee, 2000; Monica & Ardizzoia, 2007; Halcrow, 2009; Viciano-Chumillas *et al.*, 2010; Klingele *et al.*, 2009). Numerous studies of the synthesis and structure of transition-metal complexes such as Cu, Fe, Co, Ni, and Zn with pyrazole ligands indicate such compounds exhibit promising properties (Evans *et al.*, 2004; Kirthan *et al.*, 2020; Govor *et al.*, 2012; Kulkarni *et al.*, 2011; Dias *et al.*, 2020; Naik *et al.*, 2016; Malinkin *et al.*, 2012). For example, Cu^{II} pyrazole-based complexes are very promising as antioxidants (Kupcewicz, Sobiesiak *et al.*, 2013; Chkirate *et al.*, 2019) and anti-cancer agents because of their cytotoxic activity (Kupcewicz, Ciolkowski *et al.*, 2013; Aljuhani *et al.*, 2021; Santini *et al.*, 2014). Iron pyrazole-containing complexes have extraordinary electronic properties (Kulmaczewski *et al.*, 2021; Olguín & Brooker, 2011) and catalytic activity in the hydrosilylation of organocarbonyl substrates (Lin *et al.*, 2018). Cobalt complexes with pyrazole ligands are used as catalyst precursors for the peroxidative oxidation of cyclohexane (Silva *et al.*, 2014) and have useful optical and photoluminescence properties (Direm *et al.*, 2021). Zinc complexes with pyrazoles also exhibit anti-oxidative activity (Barta Holló *et al.*, 2022) and have useful luminescent properties (Li *et al.*, 2004; Singh *et al.*, 2009). The study of the synthesis, structure and properties of nickel complexes with pyrazoles is also important. Nickel(II) pyrazolate complexes can be synthesized by the reaction between

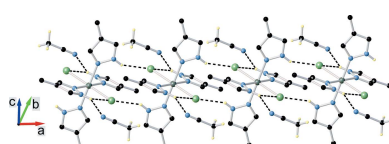
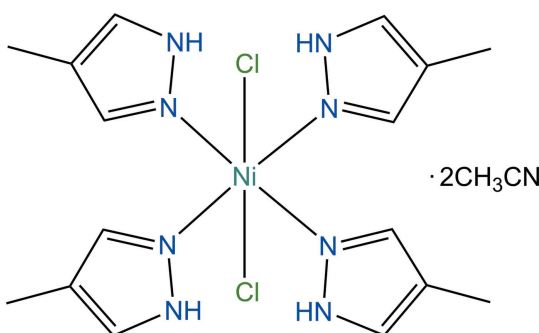


Table 1Selected geometric parameters (\AA , $^\circ$).

Ni1–N3	2.091 (2)	Ni1–Cl1	2.4581 (6)
Ni1–N1	2.112 (2)		
N3–Ni1–N3 ⁱ	180.0	N3–Ni1–Cl1 ⁱ	90.57 (6)
N3 ⁱ –Ni1–N1 ⁱ	88.18 (9)	N1 ⁱ –Ni1–N1	180.0
N3 ⁱ –Ni1–N1	91.82 (9)	N1–Ni1–Cl1	89.91 (6)
N3–Ni1–N1 ⁱ	91.83 (9)	N1 ⁱ –Ni1–Cl1	90.09 (6)
N3–Ni1–N1	88.17 (9)	N1–Ni1–Cl1 ⁱ	90.09 (6)
N3 ⁱ –Ni1–Cl1 ⁱ	89.43 (6)	N1 ⁱ –Ni1–Cl1 ⁱ	89.91 (6)
N3 ⁱ –Ni1–Cl1	90.57 (6)	Cl1 ⁱ –Ni1–Cl1	180.0
N3–Ni1–Cl1	89.43 (6)		

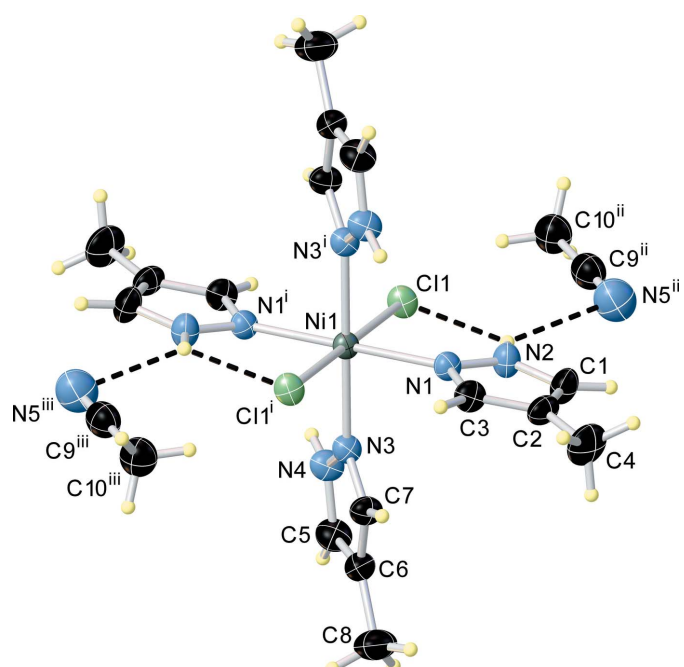
Symmetry code: (i) $-x + 1, -y + 1, -z + 2$.

nickel(II) salts and pyrazoles in water or organic solvents (Nicholls & Warburton, 1970; Sun *et al.*, 2002; Malecka *et al.*, 2001; Chen *et al.*, 2009). Nickel complexes incorporating pyrazole-based ligands are used for ethylene dimerization (Wang *et al.*, 2015) or polymerization (Nelana *et al.*, 2004; Moreno-Lara *et al.*, 2015). Mononuclear nickel(II) coordination compounds with pyrazoles show anticancer activity. The cytotoxic and apoptotic effects of such compounds suggested that they could be good candidates for further pharmacological research in the field of the development of effective anticancer agents (Gogoi *et al.*, 2019; Sobiesiak *et al.*, 2011). There is also a report on the activation of some organonitriles by transition-metal centers, such as Ni, toward nucleophilic addition of pyrazole (Hsieh *et al.*, 2009). Ni^{II} complexes can activate the pyrazole-nitrile coupling reaction. As part of our continuing interest in multifunctional transition-metal complexes with pyrazole ligands, we report herein the synthesis and crystal structure of a new mononuclear octahedral nickel(II) coordination compound based on 4-methyl-1*H*-pyrazole.



2. Structural commentary

The title compound has a molecular crystal structure, which is built-up from neutral monomeric $[\text{NiCl}_2(\text{4-MeHpz})_4]$ units (Fig. 1) and acetonitrile as interstitial molecules in a 1:2 ratio. All the components of the structure are associated *via* intermolecular N–H···N and C–H···N hydrogen bonds. Intramolecular N–H···N hydrogen bonding is also observed. The Ni^{II} ion displays a distorted octahedral coordination environment formed by four pyridine-like nitrogen atoms of 4-MeHpz ligands in the equatorial positions with Ni1–N1 =

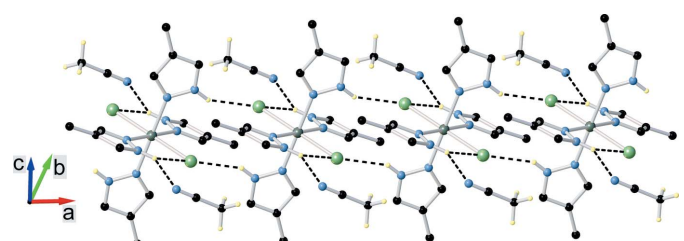
**Figure 1**

The molecular structure of the title compound with displacement ellipsoids drawn at the 50% probability level. Hydrogen-bond parameters are given in Table 2. Symmetry codes: (i) $1 - x, 1 - y, 2 - z$; (ii) $-1 + x, 1 + y, z$; (iii) $2 - x, -y, 2 - z$.

2.112 (2) \AA and Ni1–N3 = 2.092 (2) \AA bond distances and two Cl[−] anions in axial positions with an Ni1–Cl1 distance of 2.4581 (6) \AA . Selected bond lengths and bond angles are given in Table 1. The orientation of the pyrazole ligands around the metal ion is different, as indicated by the plane-to-plane angles of pyrazole rings. Two pyrazole ring planes are almost perpendicular to the NiN₄ equatorial plane [86.6 (1) $^\circ$] whereas two other pyrazole rings are less tilted [43.9 (1) $^\circ$]. The complex has an NiCl_2L_4 structure with a *trans* arrangement of the ligands and crystallographically imposed centrosymmetry.

3. Supramolecular features

The crystal structure is built up from the parallel packing of discrete supramolecular chains running along the *a*-axis direction with an Ni···Ni separation of 6.9625 (4) \AA . A perspective view of a chain is depicted in Fig. 2. Within the chain, the complex molecules interact through N–H···Cl

**Figure 2**

View of the one-dimensional supramolecular architecture in the crystal structure of the title compound.

Table 2
Hydrogen-bond geometry (\AA , $^\circ$).

$D-\text{H}\cdots A$	$D-\text{H}$	$\text{H}\cdots A$	$D\cdots A$	$D-\text{H}\cdots A$
N2—H2···N5 ⁱⁱ	0.86	2.60	3.217 (4)	130
N2—H2···Cl1	0.86	2.50	3.088 (3)	127
N4—H4···Cl1 ⁱⁱⁱ	0.86	2.45	3.217 (2)	149
C5—H5···N5 ^{iv}	0.93	2.74	3.5785 (2)	150

Symmetry codes: (ii) $x - 1, y + 1, z$; (iii) $-x, -y + 1, -z + 2$; (iv) $x - 1, y, z$.

hydrogen bonds, while the association with the interstitial acetonitrile molecules occurs via $\text{N}-\text{H}\cdots\text{N}$ hydrogen bonds. The geometric parameters of the hydrogen bonds are given in Table 2.

4. Hirshfeld surface analysis

The Hirshfeld surface analysis was performed and the associated two-dimensional fingerprint plots were generated using *Crystal Explorer 17.5* software (Spackman *et al.*, 2021), with a standard resolution of the three-dimensional d_{norm} surfaces plotted over a fixed color scale of -0.3714 (red) to 2.0459 (blue) a.u. There are six red spots on the d_{norm} surface (Fig. 3). The dark-red spots arise from interatomic contacts less than the sum of the corresponding van der Waals radii and represent negative d_{norm} values on the surface, while the other weaker intermolecular interactions appear as light-red spots. The Hirshfeld surfaces mapped over d_{norm} are shown for the $\text{H}\cdots\text{H}$, $\text{H}\cdots\text{N}/\text{N}\cdots\text{H}$, $\text{H}\cdots\text{C}/\text{C}\cdots\text{H}$, and $\text{H}\cdots\text{Cl}/\text{Cl}\cdots\text{H}$ contacts. The Hirshfeld surface representations with the function d_{norm} , which were plotted onto the surface for interactions mentioned above, the overall two-dimensional fingerprint plot, and the decomposed two-dimensional fingerprint plots for the several interactions are given in Fig. 4. The most significant contributions to the overall crystal packing are from $\text{H}\cdots\text{H}$ (62.1%), $\text{H}\cdots\text{N}/\text{N}\cdots\text{H}$ (13.7%), $\text{H}\cdots\text{C}/\text{C}\cdots\text{H}$ (13.4%), and $\text{H}\cdots\text{Cl}/\text{Cl}\cdots\text{H}$ (10.1%). There is also a small contribution from weak $\text{Cl}\cdots\text{C}/\text{C}\cdots\text{Cl}$ (0.2%) and $\text{C}\cdots\text{C}$ (0.4%) intermolecular contacts. These contacts are not visible

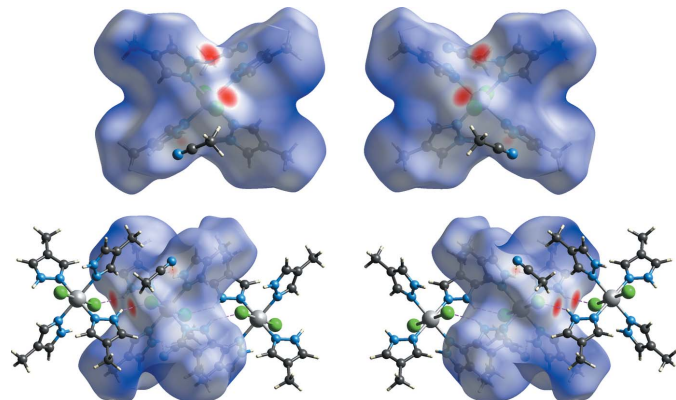


Figure 3

Two projections of Hirshfeld surfaces mapped over d_{norm} showing the intermolecular interactions within the molecule. The N4—H4···Cl1 and N2—H2···N5 contacts are shown as pink and yellow dashed lines, respectively.

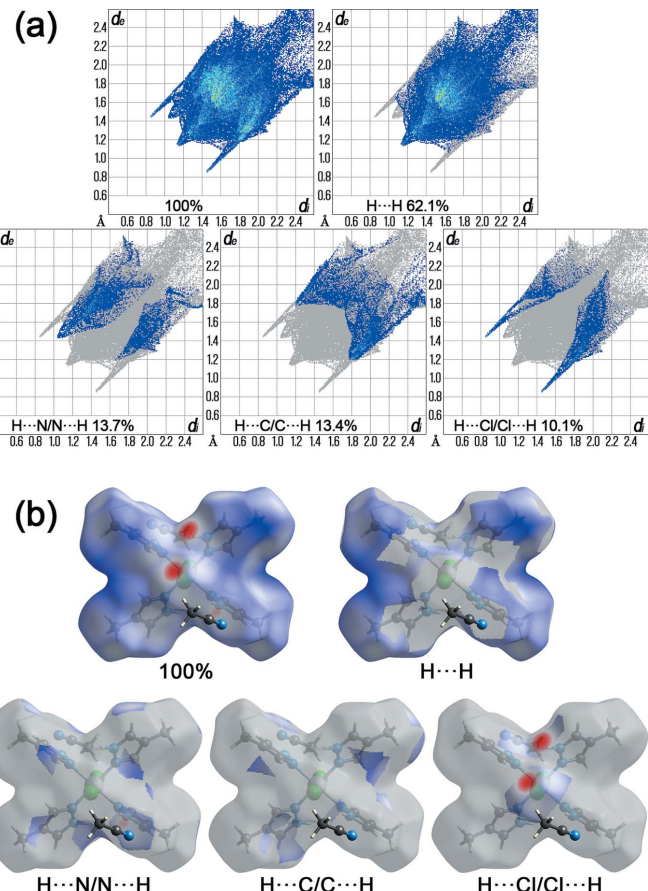


Figure 4

(a) The Hirshfeld surface representations with the function d_{norm} plotted onto the surface for selected interactions and (b) two-dimensional fingerprint plots for the title compound, showing the contributions of different types of interactions.

as red spots on the Hirshfeld surface. The $\text{H}\cdots\text{H}$ contacts are located in the middle region of the two-dimensional fingerprint plot, while $\text{H}\cdots\text{Cl}/\text{Cl}\cdots\text{H}$ contacts form sharp wings on the sides of the corresponding two-dimensional plot.

5. Database survey

A search of the Cambridge Structural Database (CSD version 5.43, November 2021; Groom *et al.*, 2016) for the $\text{Ni}(\text{C}_3\text{HN}_2)_4$ moiety (C_3HN_2 is the skeleton of pyrazole ring which is coordinated in a monodentate way) gave 60 hits while the fragment $\text{Ni}(\text{C}_3\text{HN}_2)_4X_2$, where X is any halogen, gave 20 hits (complexes with Cl and Br were found). Most similar to the title compound are the mononuclear nickel(II) pyrazole-based complexes AZEREC (Nelana *et al.*, 2004) and BOGFIN (Tao *et al.*, 2008). These complexes also crystallized in the triclinic $P\bar{1}$ space group and have similar crystal packings. Other pyrazole-containing complexes are BRTPNI (Mighell *et al.*, 1969), MUWFER (Serpas *et al.*, 2016), NIPYRA (Reimann *et al.*, 1967), NIPYRA01 (Helmholdt *et al.*, 1987), SAGBAH (Akkurt *et al.*, 2020) and SANSUW (Michaud *et al.*, 2005), which crystallized in the monoclinic crystal system and,

accordingly, have different crystal structures. In addition, all of the above pyrazole-based complexes with terminal chlorine ligands have similar geometric parameters. Finally, the central nickel atom has an octahedral geometric environment in all cases.

6. Synthesis and crystallization

The title compound was obtained by the reaction of 4-MeHpz (1.7 mmol, 0.14g) with $\text{NiCl}_2 \cdot 6\text{H}_2\text{O}$ (0.84mmol, 0.2 g) in acetonitrile (10 ml). The mixture of solid starting materials was stirred for 8 h at room temperature and the resultant green-blue solution was then filtered. Light-blue crystals of $[\text{NiCl}_2(\text{C}_4\text{H}_6\text{N}_2)_4] \cdot 2\text{CH}_3\text{CN}$ were obtained upon slow evaporation of the solvent over two weeks. CHN elemental analysis: calculated for $\text{NiCl}_2(\text{C}_4\text{H}_6\text{N}_2)_4$: C 41.95, H 5.28, N 24.46%; found: C 41.79, H 5.07, N 24.78%. The IR spectra of the starting 4-methyl-1*H*-pyrazole and clear, light-blue crystals of the title coordination compound are given in the supporting information for this article. The synthesis can be described by the following reaction: $\text{NiCl}_2 \cdot 6\text{H}_2\text{O} + 4\text{C}_4\text{H}_6\text{N}_2 + 2\text{CH}_3\text{CN} = [\text{NiCl}_2(\text{C}_4\text{H}_6\text{N}_2)_4] \cdot 2\text{CH}_3\text{CN} + 6\text{H}_2\text{O}$.

7. Refinement

Crystal data, data collection and structure refinement details are summarized in Table 3. H atoms were placed in calculated positions [C—N = 0.86 Å, C—H = 0.93 Å (0.96 Å for C-methyl)] and refined as riding with $U_{\text{iso}}(\text{H}) = 1.2U_{\text{eq}}(\text{C}, \text{N})$ or $1.5U_{\text{eq}}(\text{C}-\text{methyl})$. Reflections with $(\Delta F^2/\text{esd}) > 10$ were omitted from the refinement.

Funding information

Funding for this research was provided by: Ministry of Education and Science of Ukraine (grant No. 22BF037-09).

References

Table 3 Experimental details.	
Crystal data	
Chemical formula	$[\text{NiCl}_2(\text{C}_4\text{H}_6\text{N}_2)_4] \cdot 2\text{C}_2\text{H}_3\text{N}$
M_r	540.15
Crystal system, space group	Triclinic, $P\bar{1}$
Temperature (K)	293
a, b, c (Å)	6.9625 (4), 9.8482 (8), 11.0920 (12)
α, β, γ (°)	74.417 (8), 81.495 (6), 71.191 (6)
V (Å ³)	691.92 (10)
Z	1
Radiation type	Mo $K\alpha$
μ (mm ⁻¹)	0.92
Crystal size (mm)	0.2 × 0.15 × 0.03
Data collection	
Diffractometer	Xcalibur, Eos
Absorption correction	Multi-scan (<i>CrysAlis PRO</i> ; Rigaku OD, 2021)
T_{\min}, T_{\max}	0.795, 1.000
No. of measured, independent and observed [$I > 2\sigma(I)$] reflections	5491, 3161, 2500
R_{int}	0.031
(sin θ/λ) _{max} (Å ⁻¹)	0.691
Refinement	
$R[F^2 > 2\sigma(F^2)], wR(F^2), S$	0.047, 0.130, 1.03
No. of reflections	3161
No. of parameters	154
H-atom treatment	H-atom parameters constrained
$\Delta\rho_{\text{max}}, \Delta\rho_{\text{min}}$ (e Å ⁻³)	0.57, -0.45
Computer programs:	
<i>CrysAlis PRO</i> (Rigaku OD, 2021), <i>SHELXT2018/2</i> (Sheldrick, 2015a), <i>SHELXL2018/3</i> (Sheldrick, 2015b) and <i>OLEX2</i> (Dolomanov <i>et al.</i> , 2009).	
Gogoi, A., Dutta, D., Verma, A. K., Nath, H., Frontera, A., Guha, A. K. & Bhattacharyya, M. K. (2019). <i>Polyhedron</i> , 168 , 113–126.	
Govor, E. V., Chakraborty, I., Piñero, D. M., Baran, P., Sanakis, Y. & Raptis, R. G. (2012). <i>Polyhedron</i> , 45 , 55–60.	
Groom, C. R., Bruno, I. J., Lightfoot, M. P. & Ward, S. C. (2016). <i>Acta Cryst. B</i> , 72 , 171–179.	
Halcrow, M. A. (2009). <i>Dalton Trans.</i> pp. 2059–2073.	
Helmholdt, R. B., Hinrichs, W. & Reedijk, J. (1987). <i>Acta Cryst. C</i> , 43 , 226–229.	
Hsieh, C.-C., Lee, C.-J. & Horng, Y.-C. (2009). <i>Organometallics</i> , 28 , 4923–4928.	
Kirthan, B. R., Prabhakara, M. C., Naik, H. S. B., Nayak, P. H. A. & Naik, E. I. (2020). <i>Chem. Data Collect.</i> 29 , 100506.	
Klingele, J., Dechert, S. & Meyer, F. (2009). <i>Coord. Chem. Rev.</i> 293 , 2698–2741.	
Kulkarni, N. V., Kamath, A., Budagumpi, S. & Revankar, V. K. (2011). <i>J. Mol. Struct.</i> 1006 , 580–588.	
Kulmaczewski, R., Bamiduro, F., Shahid, N., Cespedes, O. & Halcrow, M. A. (2021). <i>Chem. Eur. J.</i> 27 , 2082–2092.	
Kupcewicz, B., Ciolkowski, M., Karwowski, B. T., Rozalski, M., Krajewska, U., Lorenz, I.-P., Mayer, P. & Budzisz, E. (2013). <i>J. Mol. Struct.</i> 1052 , 32–37.	
Kupcewicz, B., Sobiesiak, K., Malinowska, K., Koprowska, K., Czyz, M., Keppler, B. & Budzisz, E. (2013). <i>Med. Chem. Res.</i> 22 , 2395–2402.	
Li, J., Zhou, J.-H., Li, Y.-Z., Weng, L.-H., Chen, X.-T., Yu, Z. & Xue, Z. (2004). <i>Inorg. Chem. Commun.</i> 7 , 538–541.	
Lin, H.-J., Lutz, S., O'Kane, C., Zeller, M., Chen, C.-H., Al Assil, T. & Lee, W.-T. (2018). <i>Dalton Trans.</i> 47 , 3243–3247.	
Małecka, M., Rybarczyk-Pirek, A., Olszak, T. A., Malinowska, K. & Ochocki, J. (2001). <i>Acta Cryst. C</i> , 57 , 513–514.	
Malinkin, S. O., Penkova, L., Moroz, Y. S., Haukka, M., Maciąg, A., Gumienna-Kontecka, E., Pavlenko, V. A., Pavlova, S., Nordlander, E. & Fritsky, I. O. (2012). <i>Eur. J. Inorg. Chem.</i> 2012 , 1639–1649.	

- Michaud, A., Fontaine, F.-G. & Zargarian, D. (2005). *Acta Cryst. E* **61**, m846–m848.
- Mighell, A. D., Reimann, C. W. & Santoro, A. (1969). *Acta Cryst. B* **25**, 595–599.
- Monica, G. L. & Ardizzoia, G. A. (2007). *Prog. Inorg. Chem.* **46**, 151–238.
- Moreno-Lara, B., Carabineiro, S. A., Krishnamoorthy, P., Rodríguez, A. M., Mano, J. F., Manzano, B. R., Jalón, F. A. & Gomes, P. T. (2015). *J. Organomet. Chem.* **799–800**, 90–98.
- Mukherjee, R. (2000). *Coord. Chem. Rev.* **203**, 151–218.
- Naik, K., Nevrekar, A., Kokare, D. G., Kotian, A., Kamat, V. & Revankar, V. K. (2016). *J. Mol. Struct.* **1125**, 671–679.
- Nelana, S. M., Darkwa, J., Guzei, I. A. & Mapolie, S. F. (2004). *J. Organomet. Chem.* **689**, 1835–1842.
- Nicholls, D. & Warburton, B. A. (1970). *J. Inorg. Nucl. Chem.* **32**, 3871–3874.
- Olgún, J. & Brooker, S. (2011). *Coord. Chem. Rev.* **255**, 203–240.
- Reimann, C. W., Mighell, A. D. & Mauer, F. A. (1967). *Acta Cryst.* **23**, 135–141.
- Rigaku OD (2021). *CrysAlis PRO*. Rigaku Oxford Diffraction, Yarnton, England.
- Santini, C., Pellei, M., Gandin, V., Porchia, M., Tisato, F. & Marzano, C. (2014). *Chem. Rev.* **114**, 815–862.
- Serpas, L., Baum, R. R., McGhee, A., Nieto, I., Jernigan, K. L., Zeller, M., Ferrence, G. M., Tierney, D. L. & Papish, E. T. (2016). *Polyhedron*, **114**, 62–71.
- Sheldrick, G. M. (2015a). *Acta Cryst. A* **71**, 3–8.
- Sheldrick, G. M. (2015b). *Acta Cryst. C* **71**, 3–8.
- Silva, F. S. T., Martins, M. D. R. S., Guedes da Silva, m. F. C., Kuznetsov, M. L., Fernandes, A. R., Silva, A., Pan, C.-J., Lee, J.-F. & Pombeiro, A. J. L. (2014). *Chem. Asian J.* **9**, 1132–1143.
- Singh, U. P., Tyagi, P. & Pal, S. (2009). *Inorg. Chim. Acta*, **362**, 4403–4408.
- Sobiesiak, M., Lorenz, I.-P., Mayer, P., Woźniczka, M., Kufelnicki, A., Krajewska, U., Rozalski, M. & Budzisz, E. (2011). *Eur. J. Med. Chem.* **46**, 5917–5926.
- Spackman, P. R., Turner, M. J., McKinnon, J. J., Wolff, S. K., Grimwood, D. J., Jayatilaka, D. & Spackman, M. A. (2021). *J. Appl. Cryst.* **54**, 1006–1011.
- Sun, Y.-J., Chen, X.-Y., Cheng, P., Yan, S.-P., Liao, D.-Z., Jiang, Z.-H. & Shen, P.-W. (2002). *J. Mol. Struct.* **613**, 167–173.
- Tao, T. L., Riordan, C. G. & Yap, G. P. A. (2008). *CSD Communication* (CCDC 669874). CCDC, Cambridge, England. <https://doi.org/10.5517/ccqh1v2>
- Trofimenko, S. (1972). *Chem. Rev.* **72**, 497–509.
- Viciano-Chumillas, M., Tanase, S., de Jongh, L. J. & Reedijk, J. (2010). *Eur. J. Inorg. Chem.* pp. 3403–3418.
- Wang, T., Dong, B., Chen, Y.-H., Mao, G.-L. & Jiang, T. (2015). *J. Organomet. Chem.* **798**, 388–392.

supporting information

Acta Cryst. (2022). E78, 1156-1160 [https://doi.org/10.1107/S2056989022010362]

Crystal structure and Hirshfeld surface analysis of dichloridotetrakis(4-methyl-1*H*-pyrazole- κN^2)nickel(II) acetonitrile disolvate

Oleksandr S. Vynohradov, Yuliya M. Davydenko, Vadim A. Pavlenko, Dina D. Naumova, Sergiu Shova and Denys Petlovanyi

Computing details

Data collection: *CrysAlis PRO* (Rigaku OD, 2021); cell refinement: *CrysAlis PRO* (Rigaku OD, 2021); data reduction: *CrysAlis PRO* (Rigaku OD, 2021); program(s) used to solve structure: *SHELXT2018/2* (Sheldrick, 2015a); program(s) used to refine structure: *SHELXL2018/3* (Sheldrick, 2015b); molecular graphics: *OLEX2* (Dolomanov *et al.*, 2009); software used to prepare material for publication: *OLEX2* (Dolomanov *et al.*, 2009).

Dichloridotetrakis(4-methyl-1*H*-pyrazole- κN^2)nickel(II) acetonitrile disolvate

Crystal data

[NiCl ₂ (C ₄ H ₆ N ₂) ₄]·2C ₂ H ₃ N	Z = 1
M _r = 540.15	F(000) = 282
Triclinic, P1	D _x = 1.296 Mg m ⁻³
a = 6.9625 (4) Å	Mo K α radiation, λ = 0.71073 Å
b = 9.8482 (8) Å	Cell parameters from 1586 reflections
c = 11.0920 (12) Å	θ = 2.3–29.1°
α = 74.417 (8)°	μ = 0.92 mm ⁻¹
β = 81.495 (6)°	T = 293 K
γ = 71.191 (6)°	Plate, clear light blue
V = 691.92 (10) Å ³	0.2 × 0.15 × 0.03 mm

Data collection

Xcalibur, Eos	T_{\min} = 0.795, T_{\max} = 1.000
diffractometer	5491 measured reflections
Radiation source: fine-focus sealed X-ray tube,	3161 independent reflections
Enhance (Mo) X-ray Source	2500 reflections with $I > 2\sigma(I)$
Graphite monochromator	R_{int} = 0.031
Detector resolution: 16.1593 pixels mm ⁻¹	θ_{\max} = 29.4°, θ_{\min} = 1.9°
ω scans	h = -8→9
Absorption correction: multi-scan	k = -13→12
(CrysAlisPro; Rigaku OD, 2021)	l = -14→15

Refinement

Refinement on F^2	154 parameters
Least-squares matrix: full	0 restraints
$R[F^2 > 2\sigma(F^2)]$ = 0.047	Primary atom site location: dual
wR(F^2) = 0.130	Hydrogen site location: inferred from
S = 1.03	neighbouring sites
3161 reflections	H-atom parameters constrained

$$w = 1/[\sigma^2(F_o^2) + (0.0597P)^2 + 0.1286P]$$

$$\text{where } P = (F_o^2 + 2F_c^2)/3$$

$$(\Delta/\sigma)_{\max} < 0.001$$

$$\Delta\rho_{\max} = 0.57 \text{ e \AA}^{-3}$$

$$\Delta\rho_{\min} = -0.45 \text{ e \AA}^{-3}$$

Special details

Geometry. All esds (except the esd in the dihedral angle between two l.s. planes) are estimated using the full covariance matrix. The cell esds are taken into account individually in the estimation of esds in distances, angles and torsion angles; correlations between esds in cell parameters are only used when they are defined by crystal symmetry. An approximate (isotropic) treatment of cell esds is used for estimating esds involving l.s. planes.

Fractional atomic coordinates and isotropic or equivalent isotropic displacement parameters (\AA^2)

	<i>x</i>	<i>y</i>	<i>z</i>	$U_{\text{iso}}^*/U_{\text{eq}}$
Ni1	0.500000	0.500000	1.000000	0.03038 (17)
C3	0.7595 (4)	0.6698 (3)	0.7894 (3)	0.0418 (7)
H3	0.885178	0.600521	0.807503	0.050*
N2	0.4458 (4)	0.7836 (3)	0.7985 (2)	0.0433 (6)
H2	0.318650	0.807118	0.822630	0.052*
N3	0.4456 (3)	0.4131 (2)	0.8602 (2)	0.0357 (5)
C5	0.2833 (5)	0.3210 (4)	0.7604 (3)	0.0509 (8)
H5	0.184629	0.285430	0.742681	0.061*
C2	0.7297 (5)	0.7927 (4)	0.6882 (3)	0.0451 (7)
C7	0.5519 (4)	0.3886 (3)	0.7546 (3)	0.0423 (7)
H7	0.676277	0.406895	0.728729	0.051*
C6	0.4560 (5)	0.3325 (3)	0.6874 (3)	0.0464 (7)
C1	0.5283 (5)	0.8623 (4)	0.6981 (3)	0.0522 (8)
H1	0.458925	0.949441	0.644659	0.063*
C8	0.5300 (7)	0.2883 (5)	0.5643 (4)	0.0789 (12)
H8A	0.602413	0.184814	0.580475	0.118*
H8B	0.618933	0.343879	0.517855	0.118*
H8C	0.415733	0.308009	0.516557	0.118*
N1	0.5870 (3)	0.6636 (2)	0.8565 (2)	0.0354 (5)
C11	0.14603 (9)	0.65951 (7)	0.99696 (7)	0.0397 (2)
N4	0.2819 (3)	0.3701 (3)	0.8618 (3)	0.0433 (6)
H4	0.186829	0.373560	0.921075	0.052*
C4	0.8908 (6)	0.8343 (5)	0.5915 (4)	0.0752 (12)
H4A	1.021370	0.791110	0.626254	0.113*
H4B	0.861116	0.939785	0.568022	0.113*
H4C	0.892391	0.798492	0.518891	0.113*
C9	0.9065 (6)	0.0384 (4)	0.8290 (4)	0.0599 (9)
N5	1.0344 (5)	0.0551 (4)	0.7595 (4)	0.0803 (11)
C10	0.7409 (5)	0.0148 (4)	0.9202 (4)	0.0674 (11)
H10A	0.620906	0.035123	0.877485	0.101*
H10B	0.714797	0.079430	0.975807	0.101*
H10C	0.777646	-0.085902	0.967767	0.101*

Atomic displacement parameters (\AA^2)

	U^{11}	U^{22}	U^{33}	U^{12}	U^{13}	U^{23}
Ni1	0.0233 (2)	0.0330 (3)	0.0342 (3)	-0.01078 (19)	0.00342 (19)	-0.0069 (2)
C3	0.0322 (14)	0.0492 (18)	0.0462 (18)	-0.0196 (13)	0.0066 (13)	-0.0110 (15)
N2	0.0338 (12)	0.0407 (15)	0.0471 (15)	-0.0084 (11)	0.0012 (11)	-0.0019 (12)
N3	0.0285 (11)	0.0391 (13)	0.0412 (14)	-0.0139 (10)	0.0028 (10)	-0.0105 (11)
C5	0.0442 (17)	0.057 (2)	0.061 (2)	-0.0219 (15)	-0.0078 (16)	-0.0199 (17)
C2	0.0520 (18)	0.056 (2)	0.0330 (16)	-0.0293 (16)	0.0077 (14)	-0.0092 (14)
C7	0.0400 (15)	0.0505 (18)	0.0417 (17)	-0.0208 (13)	0.0078 (13)	-0.0160 (14)
C6	0.0565 (19)	0.0449 (19)	0.0390 (17)	-0.0168 (15)	-0.0018 (14)	-0.0104 (14)
C1	0.057 (2)	0.052 (2)	0.0391 (18)	-0.0174 (16)	-0.0001 (15)	0.0031 (15)
C8	0.109 (3)	0.085 (3)	0.056 (3)	-0.038 (3)	0.008 (2)	-0.034 (2)
N1	0.0320 (11)	0.0358 (13)	0.0383 (13)	-0.0136 (10)	0.0027 (10)	-0.0072 (11)
Cl1	0.0231 (3)	0.0415 (4)	0.0513 (5)	-0.0089 (3)	0.0037 (3)	-0.0101 (3)
N4	0.0299 (12)	0.0513 (15)	0.0537 (16)	-0.0178 (11)	0.0060 (11)	-0.0181 (13)
C4	0.079 (3)	0.092 (3)	0.056 (2)	-0.047 (2)	0.023 (2)	-0.007 (2)
C9	0.057 (2)	0.052 (2)	0.067 (3)	-0.0080 (17)	-0.011 (2)	-0.0142 (19)
N5	0.066 (2)	0.081 (3)	0.091 (3)	-0.0224 (18)	0.009 (2)	-0.022 (2)
C10	0.059 (2)	0.065 (3)	0.071 (3)	-0.0125 (19)	-0.002 (2)	-0.014 (2)

Geometric parameters (\AA , $^\circ$)

Ni1—N3	2.091 (2)	C2—C4	1.511 (4)
Ni1—N3 ⁱ	2.092 (2)	C7—H7	0.9300
Ni1—N1	2.112 (2)	C7—C6	1.383 (4)
Ni1—N1 ⁱ	2.112 (2)	C6—C8	1.512 (5)
Ni1—Cl1 ⁱ	2.4581 (6)	C1—H1	0.9300
Ni1—Cl1	2.4581 (6)	C8—H8A	0.9600
C3—H3	0.9300	C8—H8B	0.9600
C3—C2	1.394 (4)	C8—H8C	0.9600
C3—N1	1.326 (3)	N4—H4	0.8600
N2—H2	0.8600	C4—H4A	0.9600
N2—C1	1.344 (4)	C4—H4B	0.9600
N2—N1	1.345 (3)	C4—H4C	0.9600
N3—C7	1.327 (4)	C9—N5	1.113 (5)
N3—N4	1.334 (3)	C9—C10	1.452 (5)
C5—H5	0.9300	C10—H10A	0.9600
C5—C6	1.365 (4)	C10—H10B	0.9600
C5—N4	1.337 (4)	C10—H10C	0.9600
C2—C1	1.350 (5)		
N3—Ni1—N3 ⁱ	180.0	C6—C7—H7	124.0
N3 ⁱ —Ni1—N1 ⁱ	88.18 (9)	C5—C6—C7	104.0 (3)
N3 ⁱ —Ni1—N1	91.82 (9)	C5—C6—C8	128.1 (3)
N3—Ni1—N1 ⁱ	91.83 (9)	C7—C6—C8	127.9 (3)
N3—Ni1—N1	88.17 (9)	N2—C1—C2	108.0 (3)
N3 ⁱ —Ni1—Cl1 ⁱ	89.43 (6)	N2—C1—H1	126.0

N3 ⁱ —Ni1—Cl1	90.57 (6)	C2—C1—H1	126.0
N3—Ni1—Cl1	89.43 (6)	C6—C8—H8A	109.5
N3—Ni1—Cl1 ⁱ	90.57 (6)	C6—C8—H8B	109.5
N1 ⁱ —Ni1—N1	180.0	C6—C8—H8C	109.5
N1—Ni1—Cl1	89.91 (6)	H8A—C8—H8B	109.5
N1 ⁱ —Ni1—Cl1	90.09 (6)	H8A—C8—H8C	109.5
N1—Ni1—Cl1 ⁱ	90.09 (6)	H8B—C8—H8C	109.5
N1 ⁱ —Ni1—Cl1 ⁱ	89.91 (6)	C3—N1—Ni1	134.1 (2)
Cl1 ⁱ —Ni1—Cl1	180.0	C3—N1—N2	104.4 (2)
C2—C3—H3	124.1	N2—N1—Ni1	120.53 (17)
N1—C3—H3	124.1	N3—N4—C5	111.9 (3)
N1—C3—C2	111.8 (3)	N3—N4—H4	124.0
C1—N2—H2	124.3	C5—N4—H4	124.0
C1—N2—N1	111.4 (2)	C2—C4—H4A	109.5
N1—N2—H2	124.3	C2—C4—H4B	109.5
C7—N3—Ni1	131.41 (19)	C2—C4—H4C	109.5
C7—N3—N4	104.5 (2)	H4A—C4—H4B	109.5
N4—N3—Ni1	124.12 (18)	H4A—C4—H4C	109.5
C6—C5—H5	126.2	H4B—C4—H4C	109.5
N4—C5—H5	126.2	N5—C9—C10	179.3 (5)
N4—C5—C6	107.6 (3)	C9—C10—H10A	109.5
C3—C2—C4	126.4 (3)	C9—C10—H10B	109.5
C1—C2—C3	104.3 (3)	C9—C10—H10C	109.5
C1—C2—C4	129.3 (3)	H10A—C10—H10B	109.5
N3—C7—H7	124.0	H10A—C10—H10C	109.5
N3—C7—C6	112.1 (3)	H10B—C10—H10C	109.5
Ni1—N3—C7—C6	-178.4 (2)	C1—N2—N1—Ni1	-170.4 (2)
Ni1—N3—N4—C5	179.1 (2)	C1—N2—N1—C3	0.0 (3)
C3—C2—C1—N2	-0.5 (4)	N1—C3—C2—C1	0.5 (4)
N3—C7—C6—C5	-1.2 (4)	N1—C3—C2—C4	-179.4 (3)
N3—C7—C6—C8	-178.9 (3)	N1—N2—C1—C2	0.3 (4)
C2—C3—N1—Ni1	168.1 (2)	N4—N3—C7—C6	1.0 (3)
C2—C3—N1—N2	-0.3 (3)	N4—C5—C6—C7	0.8 (4)
C7—N3—N4—C5	-0.5 (3)	N4—C5—C6—C8	178.5 (3)
C6—C5—N4—N3	-0.3 (4)	C4—C2—C1—N2	179.4 (3)

Symmetry code: (i) $-x+1, -y+1, -z+2$.

Hydrogen-bond geometry (\AA , °)

D—H···A	D—H	H···A	D···A	D—H···A
N2—H2···N5 ⁱⁱ	0.86	2.60	3.217 (4)	130
C10 ⁱⁱ —H10C ^{vi} ···Cl1	0.96	2.94	3.697 (3)	137
N2—H2···Cl1	0.86	2.50	3.088 (3)	127
N4—H4···Cl1 ⁱⁱⁱ	0.86	2.45	3.217 (2)	149

C10 ⁱ —H10B ⁱ ···Cl1	0.96	3.12	3.8958 (3)	139
C5—H5···N5 ^{iv}	0.93	2.74	3.5785 (2)	150

Symmetry codes: (i) $-x+1, -y+1, -z+2$; (ii) $x-1, y+1, z$; (iii) $-x, -y+1, -z+2$; (iv) $x-1, y, z$.